Indian Journal of Chemical Technology
Vol. 26, January 2019, pp. 52-68

Removal of crystal violet and methylene blue dyes using Acacia Nilotica sawdust activated carbon

Tripti B Gupta[1] & Dilip H Lataye*[,2]

[1]Department of Civil Engineering, Shri Randeobaba college of Engineering and Managment , Nagpur 440 013, India.

[2]Department of Civil Engineering, Visvesvaraya National Institute of Technology, Nagpur 440 010, India.

E-mail: dhlataye@civ.vnit.ac.in,

Received 18 January 2017; accepted 9 March 2018

Removal of crystal violet dye (CV) and methylene blue dye (MB) from aqueous solution using activated carbon prepared from Acacia Nilotica sawdust (ACS) has been reported. The physico-chemical properties of ACS such as surface morphology, surface area, pore volume and composition are determined by proximate, BET, SEM and FTIR analyses. Batch experiments are performed to see the effect of different parameters like adsorbent dose, *pH*, contact time, initial dye concentration and temperature for CV and MB removal. The kinetic studies are carried out using pseudo first and second order kinetic models. To examine the nature of adsorption, to find and optimize the best-fit isotherm, Langmuir, Freundlich, Redlich-Peterson and Radke-Prausnitz isotherm equations along with ARE, MPSD and HYBRID error functions are used. The adsorption of CV and MB dyes onto ACS follows Redlich-Peterson isotherm and second order kinetic model. The maximum removal CV and MB is found to be 99.64% and 99.96% for the concentration of 50 mg/L and 41.71% and 95.14% for the concentration of 500 mg/L, respectively. The optimum adsorbent dosage for CV and MB are found to be 8 g/L and 10 g/L respectively with 1 h contact time at 303 K temperature. The thermodynamic effect of CV and MB onto ACS show the endothermic nature of sorption.

Keywords: Adsorption, Cristal violet dye, Methylene blue dye, Isotherms, Kinetics, Thermodynamics.

Today, environmental pollution is prominently increasing due to discharge of dyes from various dye-bearing industries, dyestuff manufacturing, textile industries, printing, pharmaceutical, food industries etc. It has become an important issue for the developing and emerging countries. Dyestuff discharges are unpleasant from environmental aesthetic point of view. They obstruct the photosynthesis process by interfering free passage, absorption and reflection of light and thereby causing severe harms and disturbance in the ecological balance of the aquatic life and receiving waters. Most of these dyes impart toxicity to the aquatic organisms and human beings and cause hazard to the environment. It is reported that colour is the first major contaminant to be identified in the wastewater[1]. It is estimated and predicated that about 2% of the dye effluents are discharged from manufacturing sectors, while 10% were discharged from textile and other related industries[2]. Discharge of these dyes into water bodies adversely affects the people who may use them for various domestic purposes such as drinking, bathing, washing, flushing etc. Some of the dyes can cause infections, skin problems, allergies, catagenic or mutagenic effects on living beings[3]. During the last few years, strict rules related to safe disposal and discharge of dye effluents into wastewater have been enforced. Thus, there is a must requisite of having a cost-effective and appropriately working technology for the removal of coloured impurities from the waste water. If appropriate treatment methods are not adopted, then, as its consequence, the dyes ultimately reach to the adjoining water bodies and pose risk to the marine life. For this purpose, various dyestuff removing methods have been developed and different physico-chemical processes have been applied. These include oxidation, coagulation-flocculation, photo-degradation, precipitation, membrane filtration, electro-flotation, ion-exchange etc. However, all these methods are expensive suffering from many limitations and cannot be employed by small and medium scale industries to treat the bulk quantity. Among these methods, adsorption technique appears to offer the best prospect and has been preferred as the most efficient method for the treatment of the wastewater due to its

cheap cost, simple design, less energy involvement, easy operation, negligible effects by toxic and hazardous elements and good quality treated emissions mainly for well-designed sorption systems[4]. Adsorption has been used widely in industrial process for separation, segregation and purification.

Adsorption process employs a substance that attaches the solvent molecule or the substrate to its surface. Various substitutes have been used as adsorbents for the removal and treatment of colour and dyes from the waste water. Activated carbon has been proven very efficient and is used most widely as an adsorbent in adsorption processes for the removal of various compounds like dyes, colour, pigments organic and inorganic pollutants. Commercial activated carbon (CAC) has been considered as an effective and most popular adsorbent. It has considerable potential for the treatment of wastewater due to its versatility and effectiveness like low process costs, higher surface area, comparatively efficient dye removal capacity and high adsorption capacity. But its usage is restricted because of its huge cost and associated problems related to its difficulty in regeneration. Hence there is a constant need for its substitutes. Many efforts have been made to use low cost natural and agro waste materials as substitute for CAC. It can be produced from both renewable as well as non-renewable resources with lesser cost. Some natural agricultural waste low-cost activated carbon materials obtained from renewable resources and its by-products are studied for their adsorption capacity to remove impurities from waste water. These include Sugarcane Bagasse[5], Babul Sawdust[6], Acacia Glauca Saw Dust[7], Leucaena Leucocephala waste sawdust[8], neem leaves[9], Bael (Aegle Marmelos) shell[10], soybean oil cake[11], waste orange peel[12], cocoa shell[13], banana peel[14] etc. From the literature, the authors found that the researchers have used many natural and agriculture based renewable and non-renewable by products as the adsorbent directly or by preparing activated carbon from them for treating waste water.

The present research is to remove crystal violet dye (CV) and methylene blue dye (MB) from aqueous solution using activated carbon prepared form sawdust of Acacia Nilotica (Babool tree). Sawdust is the unused small particles of wood or other material that fall from an object being sawed from sawmills which has minor economic and commercial importance. It does not involve many expenses for its collection and transportation to the desired locality. Different varieties of sawdust and their processed activated carbons have been considered to be very efficient for the removal of coloured impurities like dyes.

Crystal violet[15] is a water soluble aromatic basic dye. It is a triarylmethane dye and has antibacterial, antiseptic, antifungal, and anthelmintic properties with chemical formula as $C_{25}N_3H_{30}Cl$. Its melting point is 478K, molar mass is 407.979 g/mol and characteristic wavelength λ_{max} is 590.5 nm. The chemical structure of crystal violet dye is illustrated in Fig. 1a. According to German chemists Kern and Caro, preparation of CV involves the reaction of dimethylaniline with phosgene. It gives 4, 4' bis (dimethylamino) benzophenone (Michler's ketone) as an intermediate[16]. This was then reacted with additional dimethylaniline in the presence of phosphorus oxychloride and hydrochloric acid. The dye can also be prepared by the condensation of formaldehyde and dimethylaniline to give a leuco dye[17]. CV is basically a dark green powder with metallic lustier and when dissolved in water, the dye has a blue-violet colour. It is mostly used to dye papers and as a component of navy blue and black inks for printing, ball-point pens, and ink-jet printers. It is also used to colourise diverse products such as fertilizers, antifreezes, detergents, and leather. The dye is also used as a histological stain, particularly in Gram staining for classifying bacteria. Despite several uses of CV dye, it is also harmful to humans and if comes in contact with human beings, inhaled or ingested then may cause problems like nausea, fatigue, dizziness, headache, skin redness, irritation, cancer etc.[18].

Methylene blue[19] is a heterocyclic aromatic cationic dye with the chemical formula $C_{16}H_{18}N_3SCl$. At room temperature it appears as a solid,

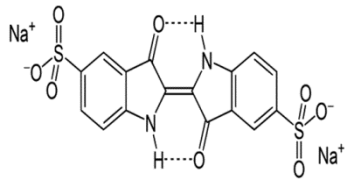

(a)

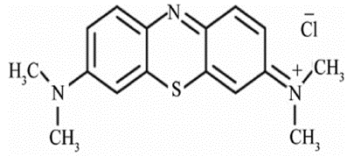

(b)

Fig. 1(a-b) — (a) Chemical structure of Crystal violet dye & (b) Chemical structure of Methylene blue dye..

dark green, odourless, powder that yields a blue solution when dissolved in water. Its molar mass is 319.85 g/mol and characteristic wavelength λ_{max} is 664 nm. The chemical structure of Methylene blue dye (MB) is illustrated in Fig. 1b. The basic dye MB is widely used in different fields, such as biology and chemistry. It is also used for dyeing, colouring paper, coating for paper stock, hair colorant, printing tannin and cotton and is also used as an antiseptic and for other medicinal purposes. Despite several uses of MB dye, it is potential carcinogen and its consumption may cause diseases like nausea, vomiting, hypertension, dizziness, staining of skin, methemoglobinemia, faecal discoloration, discoloration of urine, anaemia, cyanide poisoning, cancer etc.[20].

Thus the removal of both CV and MB dyes from wastewater demands substantial attention.

In the present work, sorption capacity of activated carbon derived from sawdust of locally available Babool tree (Scientific name: Acacia Nilotica) has been explored with an object of controlling the concentrations of crystal violet and methylene blue dyes from the aqueous solution by performing batch studies and by optimizing different physicochemical parameters. The surface chemistry, texture, area, volume and properties of the adsorbent (ACS) that has potential of adsorbing both dyes CV and MB, were studied using Brunauer–Emmett–Teller (BET) analysis, Scanning electron microscopy (SEM) and Fourier transform infrared spectroscopy (FTIR). The effect of adsorbent dose (2 g/L $\leq m \leq$ 40 g/L), initial *p*H ($2 \leq pH_0 \leq 12$), time of contact (5 min $\leq$ t $\leq$ 320 min), initial dye concentration (50 mg/L $\leq C_0 \leq$ 500 mg/L), and temperature (283K $\leq T \leq$ 323K) on the adsorption of CV and MB dyes onto ACS has been investigated. Adsorption equilibrium, adsorption thermodynamic and adsorption kinetic studies have also been evaluated. Isotherm equations like Langmuir, Freundlich, Redlich-Peterson and Radke-Prausnitz have been considered to illustrate the well describing and best suited experimental sorption isotherm data and to examine the nature of adsorption. Error analysis has also been conducted to check the accuracy of various adsorption isotherm equations.

Experimental Section

Adsorbent preparation

Though CAC are usually derived from natural resources such as coal, biomass or lignite, but more or less any carbonaceous material might be considered as pioneer for the preparation of carbon adsorbents[21]. In the present study, activated carbon derived from sawdust of Acacia Nilotica has been used as an adsorbent. The raw sawdust was first sieved to obtain a desirable size fraction between 250 μ and 500 μ as per IS 2720:1985 (IV) [22]. The obtained size fraction of raw sawdust was then washed several times with doubled distilled water (DDW) to remove containments or impurities present if any. This washed sawdust was then sun dried open to sky for about 1 day. After this, it was oven dried for about 3 h at 378K. Then about 100 g of dried sawdust was mixed with 50 mL of emparta ortho phosphoric acid (H_3PO_4, molecular weight 98 g/moL) and it was kept stand by for 1 day so as to obtain char from it. The char produced after 24 h, was then thermally activated for 1 h in a muffle furnace by maintaining the inside temperature of 673K to 723K. In order to remove traces of acid present if any, the derived activated carbon was again washed with DDW. Afterwards, the washed derived activated carbon was air dried open to sky and oven dried for 3 h in the hot air oven by maintaining inside temperature of 378K. The activated carbon so obtained was finally used as an adsorbent material for the present adsorption study.

Adsorbate preparation

All the chemicals used in the study viz., acids, alkalies, KNO_3 etc. were of analytical reagent grade. They were supplied by S.D. Fine Chemicals, Mumbai, India. The commercial crystal violet and methylene blue dyes were purchased from Upper India Scientific Cooperation Nagpur. All the solutions were prepared with DDW.

Adsorbent characterization

The physico-chemical characteristics of the ACS were determined using standard procedures. Proximate analysis, were carried out as per IS 1350:1984[23], batch adsorption studies, equilibrium studies, CV and MB dye analysis, Effect of various characteristics on adsorbent (ACS) were also found out using standard procedures.

Batch experimental programme and adsorption equilibrium study

The experimental program was performed by conducting batch adsorption studies so as to evaluate the adsorption capacity of the adsorbent on the adsorbate. The standard stock solution of 1000 mg/L was prepared by taking 1 g dye powder in 1000 mL of DDW. The subsequent concentration range of

adsorbate solutions (varied from 1 to 500 mg/L) were prepared by diluting the aqueous CV and MB stock solutions with DDW in required proportions. The solutions of 0.05, 0.1, 0.2, 0.5, 1, 1.5, 2, 3 and 5 mg/L were prepared and the standard graph of concentration versus absorbance were plotted by measuring the absorbance for both CV and MB dyes at 590.5 nm and 664 nm wavelength respectively. Absorbance was found out using UV-Vis double beam spectrophotometer. The batch adsorption studies for both dyes were carried out using temperature controlled orbital shaker incubator (REMI, Mumbai, India, Model: CIS 24-BL) and the analyses of both dyes were carried out using double beam UV-Vis Spectrophotometer (Shimadzu, Japan, Model: UV-2450). The temperature range for the studies was from 283K to 323K. All the batch studies were performed at the shaking speed of 150 revolutions per minute (RPM). For each experimental run, 50 mL aqueous solution of the known dye concentration was taken in a 250 mL stoppered conical flask containing a known mass of the adsorbent. The samples with higher concentration of CV and MB (> 0.900 absorbance) were diluted with DDW for the precise determination of dye concentrations by using linear relationship of the calibration curve.

The adsorption experiments for CV and MB dyes were carried out by adding fixed amount of adsorbent into 50 mL of related dye solution with the range of initial concentrations as 50 mg/L to 500 mg/L (at optimum *p*H) in 250 mL stoppered conical flasks to avoid evaporation of dye solution before putting into the shaking incubator and the specific temperature until it reaches to equilibrium.

The adsorption capacity (q_e) for ACS and percentage removal (%) of CV and MB dyes were calculated using the following relationships:

$$q_e = \frac{(C_0 - C_e)V}{W} \quad \ldots (1)$$

$$\%\, Removal = \frac{(C_0 - C_e)}{C_0} \times 100 \quad \ldots (2)$$

where, q_e is the amount of adsorbate adsorbed per unit weight of adsorbent at equilibrium (mg/g), C_0 is the initial concentration of dye (mg/L), C_e is the final or equilibrium concentration of dye (mg/L), V is the volume of sample (L) and W is the amount of adsorbent (g).

Results and Discussion

Characterization of Adsorbent

As adsorption is a surface based process in which there is an adhesion of ions, atoms, or molecules from a liquid or gas to an adsorbent surface. Hence, the rate and amount of adsorption are strongly reliant on surface composition, surface properties, and surface porosity of the adsorbent. The characteristics of ACS sample such as surface area, pore volumes surface morphology, and surface chemistry were determined by BET, SEM and FTIR analysis. The physico-chemical properties of ACS sample such as moisture content, volatile matter content, ash content, and fixed carbon content were analyzed for its proximate analysis. Proximate analysis of the adsorbent (ACS) was carried out as per IS 1350:1984[23]. From the analysis it is found that, the moisture content, ash content, volatile matter and fixed carbon content of ACS are 17.60, 9.60, 17.00 and 55.80% respectively. The Brunauer–Emmett–Teller (BET) analysis was carried out to determine the surface area and pore volume of ACS sample. The surface area and pore volume of ACS were determined using surface area and pore volume analyzer (Model: Smart Sorb 92/93, Make: Smart instruments Co. Pvt. Ltd. Dombivli) at 292K. The results of the analysis are given in Table 1. The Scanning Electron Microscopy (SEM) analysis explains the surface morphology and surface porosity of adsorbent. The surface of the virgin ACS and the ACS loaded with CV and MB dyes were tested at 500 X magnification using model JEOL Tokyo, Japan (JSM 6380 A) make scanning electron microscope. As all the three samples, were having nonconductive nature, they were provided with thin platinum coating using JFC 1600 JEOL Coater. Fig. 2(a) shows the SEM image of the virgin ACS. From the image of virgin ACS it can be seen that there are large number of asymmetrical and porous cavities which are accountable for the adsorption of CV and MB dyes over its surface.

Table 1 — BET analysis of ACS

Percentage of N_2 for Surface area	:	30%
Percentage of N_2 for Pore volume	:	95.01%
Room temperature	:	29 ^oC
Weight of the tube-sample	:	23.4005 g
Injected volume	:	7 cc
Surface area	:	737.76 Sq.M/g
Pore volume	:	0.2582 cc/g

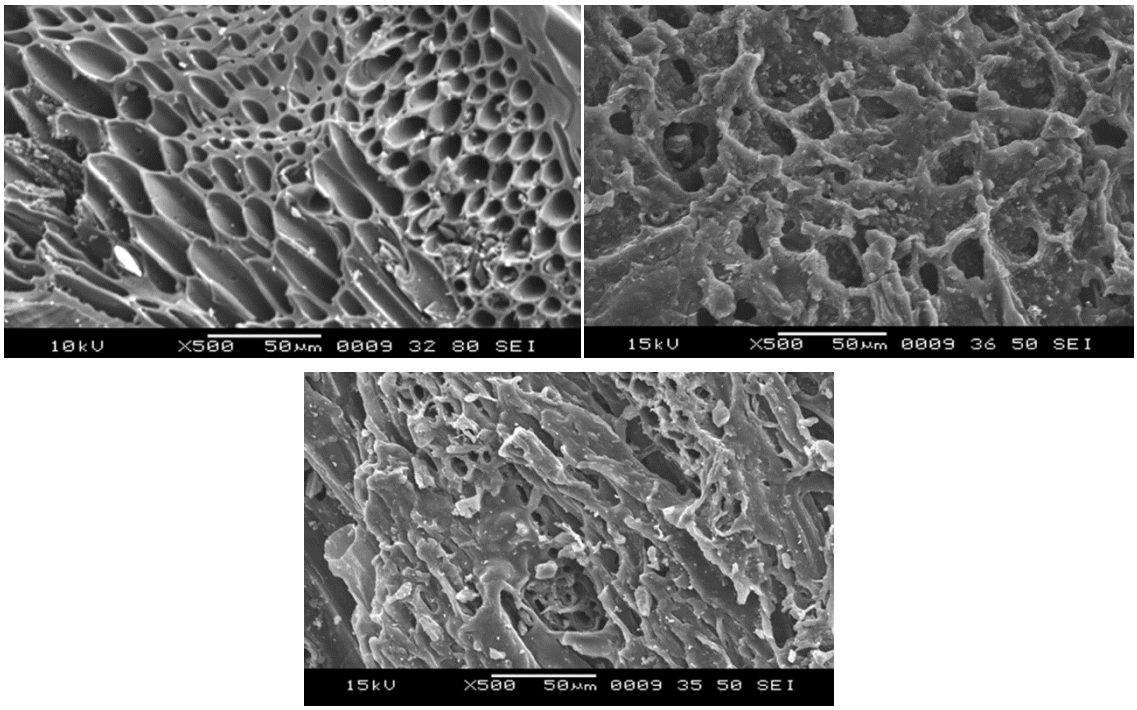

Fig. 2 (a-c) — (a) SEM image of virgin ACS sample, (b) SEM image of ACS sample loaded with CV dye and (c) SEM image of loaded ACS sample loaded with MB dye.

Fig. 2(a) also shows that these porous cavities are sufficient enough to allow the molecules of CV and MB dyes to penetrate into the lingo cellulosic honeycomb like structure and interact therein with the different surface and functional groups. Fig. 2(b and c) shows the SEM images of the ACS loaded with CV and MB respectively. From both the figures, we can say that there was distortion of pores, the porous cavities got densely packed with the respective dyes, all the voids got filled up and there was layered deposition on the surface of ACS loaded with CV and MB dyes respectively making the surface smooth and even compared with virgin ACS (Fig. 2(a)). The surface chemistry of the ACS under both virgin and loaded conditions was analyzed by Fourier Transform Infrared Spectroscopy (FTIR). Figure 3 (a, b and c) shows the FTIR spectroscopy of virgin ACS and ACS loaded with CV and MB dyes respectively in the range of 500 cm^{-1} to 4,000 cm^{-1}. The respective peaks of the graph were plotted by considering percentage transmittance (%) on ordinate and wave number (cm^{-1}) on abscissa. The spectroscopy indicates the presence of distinctive functional groups on the surface of ACS under both virgin and loaded conditions. The band stretched in the virgin ACS sample at 3,651.06 is because of the presence of -OH stretch group which slightly shifts to a range of 3,604.95 for ACS loaded by CV dye and to a range of 3651.02 cm^{-1} for ACS loaded by MB dye. The band stretched in the virgin ACS sample at 2,981.49 cm^{-1} indicates the presence of a strong C-H bond which shifts very slightly in loaded ACS sample to 2,981.46 cm^{-1} when it adsorbs the CV dye and to 2,884.65 cm^{-1} when it adsorbs the MB dye. The band stretched in the virgin ACS sample at 2,099.46 cm^{-1} indicates the presence of a weak C-C bond which does not shift when it adsorbs the CV dye and shifts slightly to 2106.30 cm^{-1} when it adsorbs the MB dye Similarly, the peak at 1,529.81 cm^{-1} for virgin ACS, 1,522.97 cm^{-1} for ACS loaded with CV and 1,597.42 cm^{-1} for ACS loaded with MB indicates the presence of alkanes and C-O groups.

Batch adsorption study

Batch study was carried out so as to study the effect of different operating parameters. Experiments were carried out in 250 mL stoppered conical flasks for removal of CV and MB dyes from aqueous solutions of known concentrations by using ACS. The effect of different parameters like adsorbent dose, initial *p*H, initial dye concentration, contact time and temperature had been studied.

Effect of adsorbent dose (m)

The effect of adsorbent dose (m_{CV} and m_{MB}) for the removal of CV and MB dyes by ACS at initial

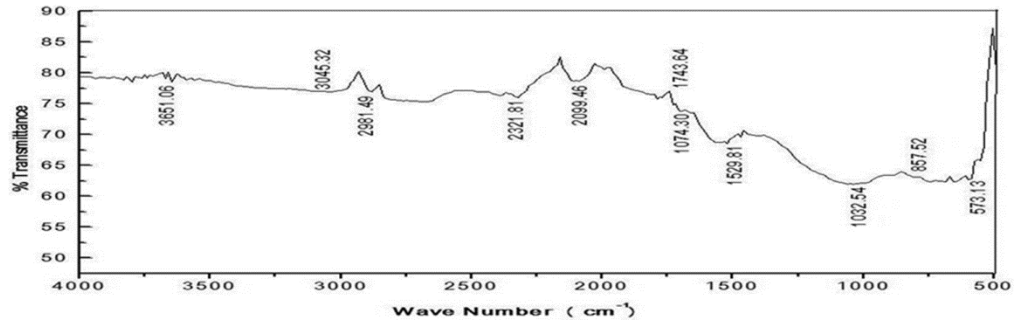

(a)

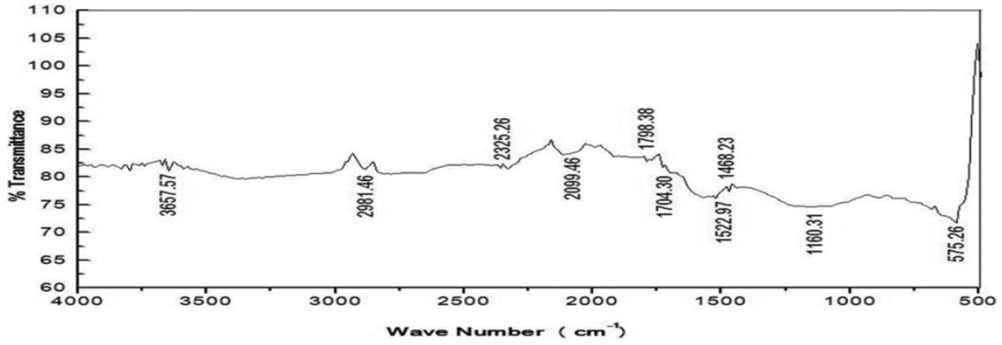

(b)

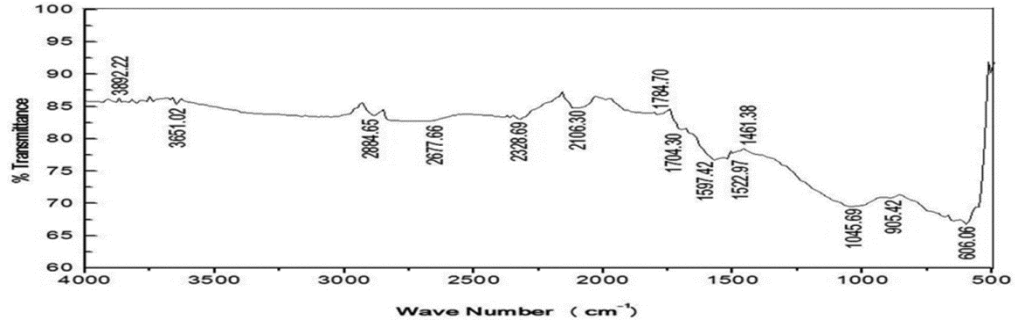

(c)

Fig. 3(a-c) — (a) FTIR spectra of virgin ACS sample, (b) FTIR spectra of ACS sample loaded with CV dye and (c) FTIR spectra of ACS sample loaded with MB dye.

concentration C_0= 50 mg/L is shown in Fig. 4. It can be seen that the CV and MB dyes removal increases rapidly with an increase in adsorbent dose of ACS up to 8 g/L and 10 g/L respectively. Further increasing the adsorbent dose from 8 g/L for CV and 10 g/L for MB to 20 g/L for both CV and MB results in a marginal increment in % removal of CV and MB and beyond that, the removal of dye is almost constant and unaffected by an increase of adsorbent dose. Thus it can be seen that CV and MB dyes removal increases up to a certain limit and then it becomes quite consistent. Optimum '*m*' for removal of ACS by CV dye was found to be about 8 mg/L and by MB dye was found to be about 10 mg/L. An increase in the adsorption with the adsorbent dosage can be accredited to availability of larger surface area at initial phase of adsorption and of more adsorption sites[24]. Further, in all the cases, equilibrium was established to be achieved more quickly at smaller adsorbent dosage. However, the rate of adsorption decreases with the increase in the adsorption dosage. Thus, at the dose of 8 g/L for CV and 10 g/L for MB of ACS, the solution approaches to equilibrium. Thus, the optimum '*m*' of ACS for CV and MB removal can be taken as 8 g/L and 10 g/L respectively.

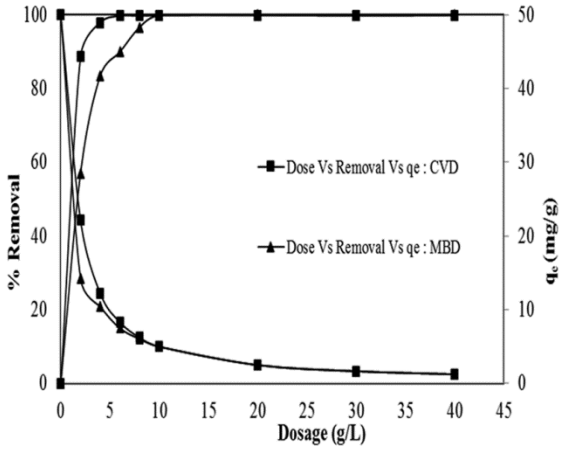

Fig. 4 — Effect of Dose on the adsorption of CV and MB on adsorption capacity by ACS (C_0 = 50 mg/L, V= 50 mL, T = 303K, RPM = 150, t = 1 hour and pH_{CV}= 6.51, pH_{MB} = 6.96 (Natural)).

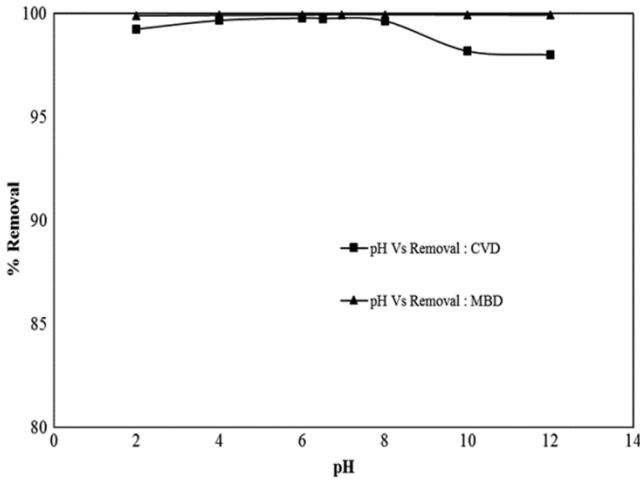

Fig. 5 — Effect of *pH* on the adsorption of CV and MB by ACS (C_0 = 50 mg/L, V = 50 mL, T = 303K, m_{CV} = 8 g/L and m_{MB} = 10 g/L, RPM = 150 and t = 1 hour).

Effect of Initial pH (pHo)

The effect of the initial *p*H of the CV and MB solution on the adsorption capacity of ACS was investigated at 50 mg/L initial dye concentration, 8 g/L m_{CV} and 10 g/L m_{MB}, 1 h of contact time, 303K temperature and 150 RPM stirring speed. The *p*H of the CV and MB solution varied between 2 and 12. The *p*H of any solution is an important parameter for adsorption that affects the surface charge of the adsorbent from aqueous solution as well as the degree of ionization of the adsorbate during reaction. The hydrogen and hydroxyl ions are adsorbed quite strongly on the adsorbent surface and, therefore, the adsorption of other ions and molecules is affected by the *p*H of the solution. The change of *p*H affects the adsorptive system process through dissociation of functional groups of the adsorbent. This subsequently leads to a swing in equilibrium properties and kinetics of the adsorption process[25]. It is a common observation that the surface adsorbs anions favourably at lower *p*H range due to presence of hydrogen (H^+) ions, whereas, the surface is active for the adsorption of cations at higher *p*H range due to the deposition of hydroxyl (OH^-) ions. The colour was almost stable at around natural *p*H (pH_{CV} = 6.51 and pH_{MB} = 6.96) shown in Fig. 5 for ACS, therefore further experiments were conducted at natural *pH* 6.51 for CV and 6.95 for MB. The *p*H at which the net charge of adsorbent is equal to zero is known as point of zero charge (pH_{PZC}). The point of zero charge (pH_{PZC}) of the adsorbent (ACS) determined using solid addition method[26] was found to be 4.25. At higher *p*H range ($pH_o < pH_{PZC}$), the surface of the adsorbent (ACS) is charged negatively and the adsorption of dye molecules increases due to the electrostatic attraction between the surface (ACS) and cationic dye (CV and MB) molecules. At lower *p*H range ($pH_o<pH_{PZC}$), since the surface of the ACS is charged positively, the expected tendency is decreasing the adsorption of CV and MB dyes due to the electrostatic repulsion between cationic dye molecules and the surface of the adsorbent. However, in present study, as seen in Fig. 5, in an acidic medium the initial *p*H value of adsorption firstly increases and then reaches an initial value and then decreases. Thus during the adsorption process it was observed that the *p*H of the solution was decreased after adding the adsorbent dosage. The initial *p*H of the solution was 6.51 for CV and 6.95 for MB which has become < 6.76. The *p*H of the solution after adding adsorbent dosage decreases due to surface becoming negative by adsorbing hydroxyl (OH^-) ions from the solution[27].

Effect of contact time (t)

The effect of contact time on the removal of CV and MB dyes by ACS at C_0 = 50, 100 and 200 mg/L is shown in Fig. 6(a and b). The figure shows rapid adsorption of CV and MB in the first 15 min because of the availability of a large number of surface sites on ACS, thereafter, the adsorption rate decreases slowly and the adsorption reaches the equilibrium in 1 hour of contact time. It is found that for initial concentration, C_0 = 100 mg/L, about 62% of CV and about 90% of MB has been removed at first 15 min of contact time. The residual concentration at first 15 min and at 1 hour contact time was found to be

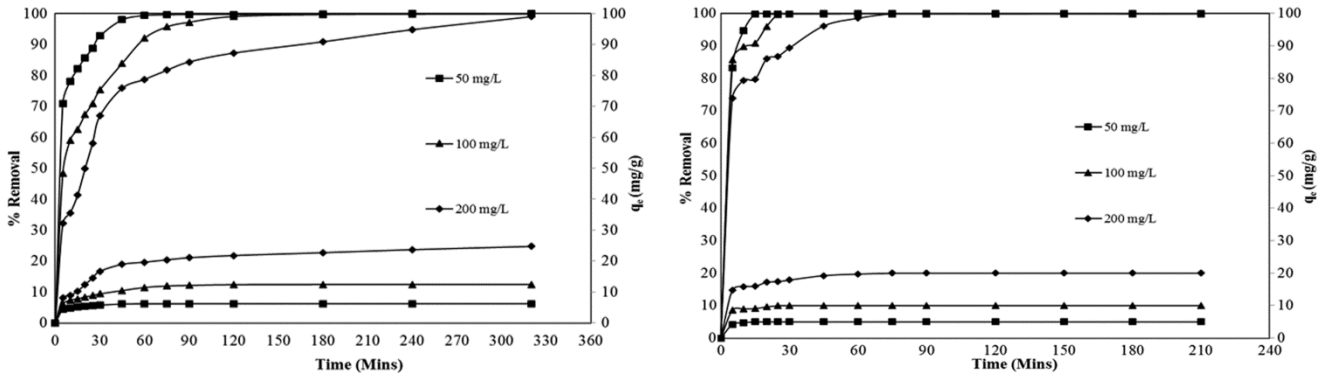

(a) (b)

Fig. 6(a-b) — (a) Effect of contact time on % removal of CV (C_0 = 50, 100 and 200 mg/L, V = 50 mL, T = 303K, m = 8 g/L, pH_0 = 6.51 and RPM = 150) & (b) Effect of contact time on % removal of MB (C_0 = 50, 100 and 200 mg/L, V = 50 mL, T = 303K, m = 10 g/L, pH_0 = 6.96 and RPM = 150).

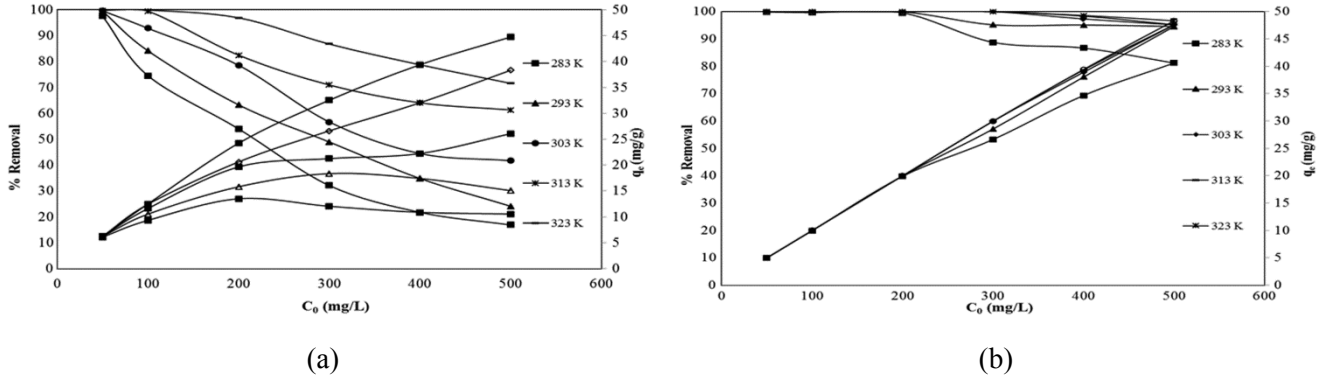

(a) (b)

Fig. 7(a-b) — (a) Effect of initial dye concentration and temperature on % removal of CV by ACS at different temperatures (C_0 = 50, 100 and 200 mg/L, V = 50 mL, m = 8 g/L, pH_0 = 6.51, RPM = 150 and t = 1 hour) & (b) Fig. 7b — Effect of initial dye concentration and temperature on % removal of MB by ACS at different temperatures (C_0 = 50, 100 and 200 mg/L, V = 50 mL, m = 10 g/L, pH_0 = 6.96, RPM = 150 and t = 1 hour).

about 37.38% and 7.97% respectively for CV and about 9.19% and 0.10% respectively for MB. While for 3 hr contact time it is found to be about 0.31% and 0.12% for CV and MB respectively. The difference between residual concentration at 15 min and 1 hour contact time was more than 8% and the difference in residual concentration at 2 hr and 3 hr contact time is less than 1%, hence a steady state approximation was assumed and a quasi-equilibrium situation was accepted at t = 1 h[24,26,28]. Further, increase in contact time showed that the CV and MB dyes removal increases slightly over those obtained for optimum contact time. Aggregation of dye molecules with the increase in contact time makes it almost impossible to diffuse deeper into the adsorbent structure at highest energy sites. This aggregation negates the influence of contact time as the voids and mesopores get filled up by respective dyes and start offering resistance to diffusion of aggregated dye molecules in the adsorbents. This is the reason behind insignificant enhancement in adsorption with contact time as compared to that in optimum time. Hence further experiments were conducted for optimum contact time only. The curves are even, continuous, smooth, single and leading to saturation. The curves also indicate that there is probable mono-layer cover of respective dye on the surface of ACS. From the Fig. 6 (a and b) it is found that the percentage removal of CV and MB is maximum at 1 h contact time, which remains constant after this time. This means that the equilibrium time for the CV and MB dyes removal by ACS is 1 h. Further all experiments were done by considering 1 h as a contact time.

Effect of initial dye concentration (C_0) and temperature (T)

The effect of initial dye concentration C_0 on the removal of CV and MB dyes by ACS is shown in Fig. 7(a and b). It is evident that the amount of CV

and MB dyes adsorbed per unit mass of adsorbent (q_e) increased with the increase in C_0, although percentage CV and MB removal decreased with the increase in C_0 as resistance to the uptake of CV and MB dyes from the solution decreases with the increase in CV and MB concentration. The rate of adsorption also increases with the increase in C_0 due to increasing driving force[24,28].

Temperature has a pronounced effect on the adsorption capacity and its dependency on adsorption is of complex nature. Fig. 7(a and b) shows the plots of adsorption isotherms, for CV-ACS and MB-ACS systems at 283, 293, 303, 313 and 323K. It shows that the absorptivity of CV and MB increases with the increase in temperature which indicates the endothermic nature of the process[29]. This increase also shows that the adsorption process may be because of chemo-sorption. Fig. 7(a and b) shows that at lower adsorbate (CV and MB) concentrations, q_e rises sharply and thereafter the increase is gradual. Since adsorption is an exothermic process, it would be likely that an increase in temperature of the adsorbate-adsorbent system would result in decreased adsorption capacity. However, if the adsorption process is controlled by the intra particle transport-pore diffusion process, then the adsorption capacity will show an increase with an increase in temperatures[30]. This is basically due to the fact that the intra particle transport-pore diffusion process is an endothermic process. With an increase in temperature, the mobility of the CV and MB ions increases and the retarding forces acting on the diffusing ions decrease, thereby increasing the adsorptive capacity of adsorbent (ACS). This increase in adsorption capacity is mainly due to an increase in number of adsorption sites caused by breakdown of certain inside bonds close to the verge of the active surface sites of the adsorbent[31]. Rise in dye sorption capability of the other adsorbents with the rise in temperature has also been described by other investigators[32].

Adsorption equilibrium study

When a solution comprising of adsorbate, comes in interaction with a solid adsorbent, molecules of adsorbate get transmitted from the solution phase to the compact solid phase until the concentration of adsorbate amongst the solution phase and the compact solid phase are in equilibrium. This is called adsorption equilibrium. Isotherms are the graphs showing distribution process of adsorption between the adsorbed phase and the solution phase at equilibrium. Various isotherm equivalences have been used to describe the equilibrium characteristics of adsorption. Fig. 8(a and b), Fig. 9(a and b), Fig. 10(a and b) and Fig. 11(a and b) shows Langmuir, Freundlich, Redlich-Peterson and Radke-Prausnitz isotherm plots for adsorption of CV and MB by ACS respectively at 283, 293, 303, 313 and 323 K. Various isotherm parameters along with linear as well as nonlinear correlation coefficients are given in Table 2.

The Langmuir isotherm assumes that dynamic equilibrium occurs between adsorbed and free gaseous molecules. The adsorption involves the attachment of only one layer to the surface i. e. only monolayer adsorption is possible onto a surface with a finite number of similar active sites undergoing adsorption. Adsorption occurs at specific homogeneous active sites within the adsorbent.

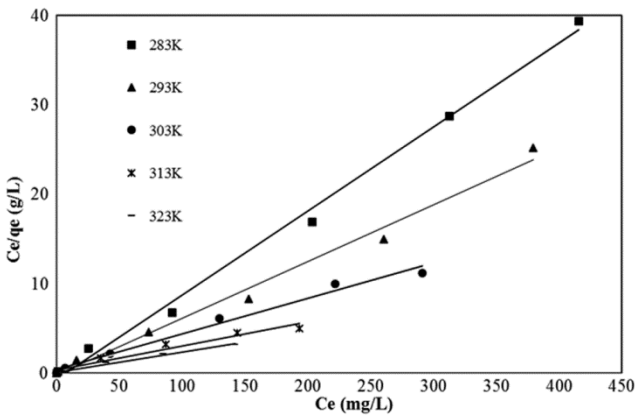

(a)

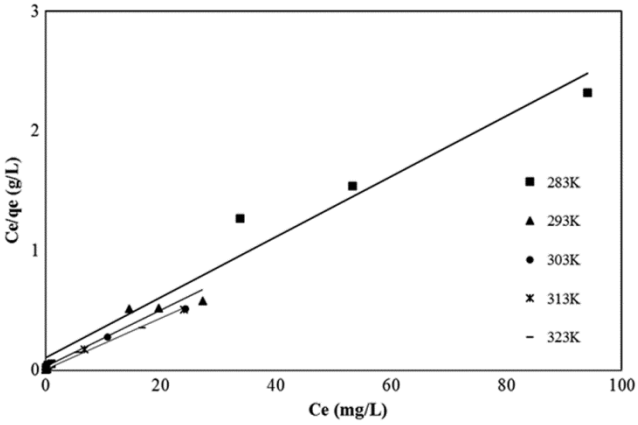

(b)

Fig. 8(a-b) — (a) Langmuir isotherm plot for removal of CV by ACS (m = 8 g/L, pH_0 = 6.51 and t = 1 hour) and (b) Langmuir isotherm plot for removal of MB by ACS (m = 10 g/L, pH_0 = 6.96 and t = 1 hour).

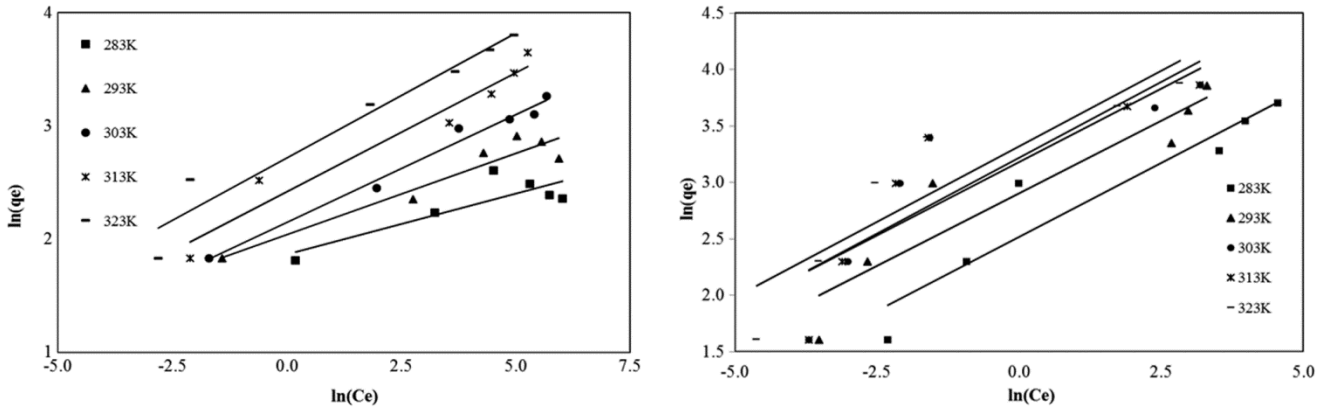

Fig. 9(a-b) — (a) Freundlich isotherm plot for removal of CV by ACS (m = 8 g/L, pH_0 = 6.51 and t = 1 hour) and (b) Freundlich isotherm plot for removal of MB by ACS (m = 10 g/L, pH_0 = 6.96 and t = 1 hour).

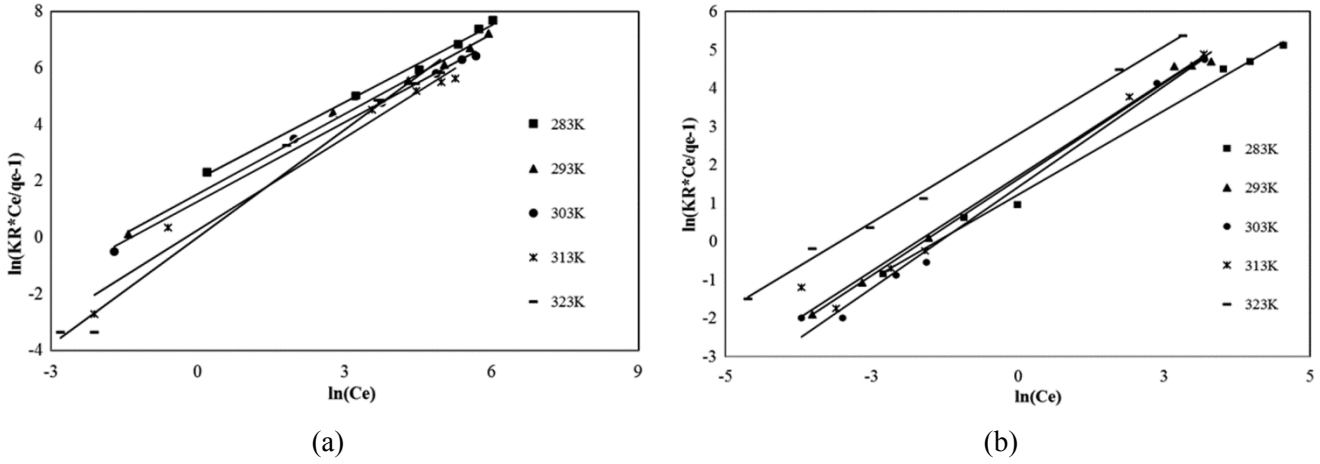

Fig. 10(a-b) — (a) Redlich-Peterson isotherm plot for removal of CV by ACS (m = 8 g/L, pH_0 = 6.51 and t = 1 hour) and (b) Redlich-Peterson isotherm plot for removal of MB by ACS (m = 10 g/L, pH_0 = 6.96 and t = 1 hour).

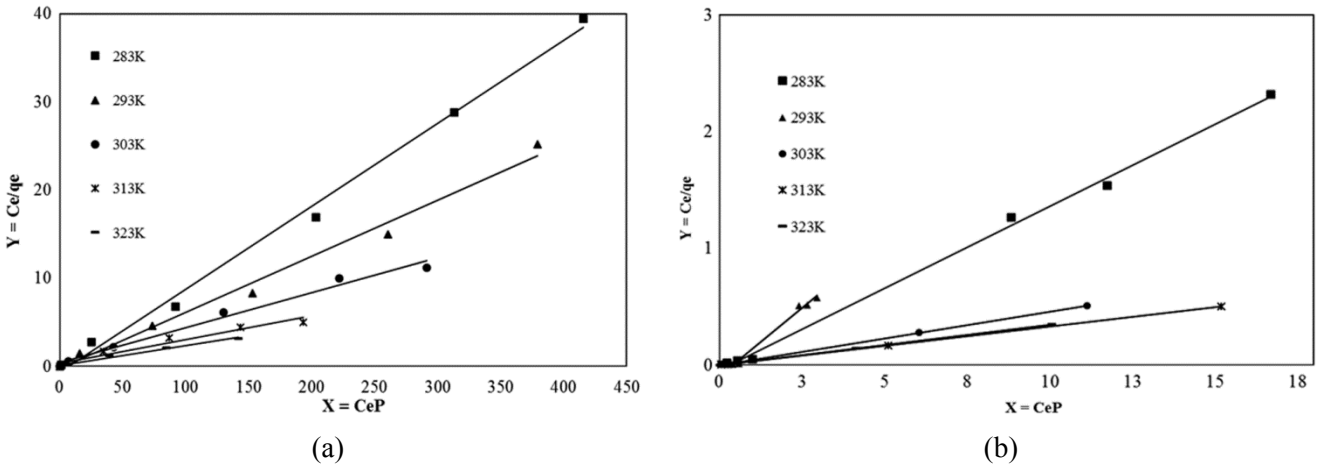

Fig. 11(a-b) — (a) Radke-Prausnitz isotherm plot for removal of CV by ACS (m = 8 g/L, pH_0 = 6.51 and t = 1 hour) and (b) Radke-Prausnitz isotherm plot for removal of MB by ACS (m = 10 g/L, pH_0 = 6.96 and t = 1 hour).

Table 2 — Isotherm parameter along with linear and non-linear correlation coefficients.

Isotherms	Constants	Temperatures (Kelvin, K)									
		283		293		303		313		323	
		CV	MB	CV	MB	CV	MB	CV	MB	CV	MB
Langmuir	q_m, mg/g	10.627	39.683	15.748	42.553	25.253	46.948	37.313	47.619	44.444	48.077
	K_L, L/mg	0.139	0.243	0.280	0.797	0.091	2.393	0.072	2.800	0.200	3.714
	R^2 (Linear)	0.995	0.969	0.988	0.928	0.986	0.992	0.956	0.997	0.988	0.995
	R^2 (Non-Linear)	0.997	0.984	0.994	0.963	0.993	0.996	0.978	0.998	0.994	0.997
	HYBRID	1.334	43.765	0.903	49.582	0.942	44.812	1.356	39.292	1.579	45.376
	MPSD	0.671	62.801	0.795	68.581	0.914	48.821	1.830	43.448	1.727	51.137
	ARE	1.334	42.201	1.417	47.164	1.344	35.256	2.496	31.184	2.163	35.719
Freundlich	K_F, L/mg	6.456	12.432	7.682	18.273	8.550	24.044	11.222	25.028	15.139	27.691
	n	9.328	3.811	6.949	3.885	5.010	3.846	6.949	3.723	4.541	3.741
	$1/n$	0.107	0.262	0.144	0.257	0.200	0.260	0.144	0.269	0.220	0.267
	R^2 (Linear)	0.722	0.894	0.915	0.874	0.983	0.748	0.951	0.752	0.947	0.823
	R^2 (Non-Linear)	0.850	0.946	0.957	0.935	0.991	0.865	0.975	0.867	0.973	0.907
	HYBRID	-0.051	-4.037	-0.038	-5.689	-0.198	-11.883	0.795	-11.897	-0.077	-8.308
	MPSD	0.098	27.429	0.076	34.164	0.036	51.679	0.407	52.282	0.159	41.621
	ARE	0.644	15.967	0.545	22.400	0.403	33.552	1.451	33.209	0.689	28.821
Redlich-Peterson	K_R, L/mg	55.0	72.461	55.0	193.9	55.0	230.0	55.0	264.5	107.0	619.9
	β	0.908	0.879	0.941	1.001	0.867	1.055	1.088	0.987	1.269	0.917
	a_R, L/mg	7.822	3.412	4.679	5.104	3.572	4.197	1.294	5.531	1.004	16.381
	R^2 (Linear)	0.995	0.995	0.996	0.997	0.994	0.991	0.977	0.976	0.981	0.997
	R^2 (Non-Linear)	0.998	0.998	0.998	0.999	0.997	0.995	0.989	0.988	0.991	0.998
	HYBRID	3.811	-1.775	3.866	-2.814	4.368	-1.457	1.389	-2.667	-5.352	0.135
	MPSD	6.415	18.676	6.284	21.449	5.287	14.678	1.556	18.918	8.416	11.929
	ARE	6.189	10.836	6.133	8.956	5.562	7.971	2.608	11.917	5.630	7.016
Radke-Prausnitz	P	1.000	0.619	1.000	0.329	1.000	0.755	1.000	0.856	1.000	0.817
	k_{RP} ((mg/g) /(mg/L)$^{1/P}$)	10.638	7.117	15.873	8.197	25.641	47.619	38.462	34.483	45.455	37.037
	K_{RP} L/g	0.139	3.252	0.279	5.545	0.090	2.625	0.070	7.250	0.196	13.500
	R^2 (Linear)	0.994	0.891	0.987	0.984	0.985	0.991	0.956	0.997	0.987	0.998
	R^2 (Non-Linear)	0.997	0.999	0.994	0.995	0.993	1.000	0.978	1.000	0.994	1.000
	HYBRID	1.329	2.281	0.865	3.975	0.877	4.784	1.239	4.880	1.496	5.061
	MPSD	0.670	1.546	0.795	2.973	0.917	4.005	1.862	4.130	1.741	4.401
	ARE	1.329	2.281	1.412	3.975	1.369	4.784	2.560	4.880	2.203	5.061

Adsorbent surface is uniform in terms of energy of adsorption. Adsorbed molecules do not interact with each other. Adsorbed molecules do not migrate on the adsorbent surface. The adsorption isotherm derived by Irving Langmuir for the adsorption of a solute from a liquid solution is given by Langmuir[33]:

$$\frac{C_e}{q_e} = \frac{C_e}{q_m} + \frac{1}{K_L q_m} \quad \text{... (3)}$$

where, C_e is equilibrium or final concentration of dye (mg/L), q_e is amount of adsorbate adsorbed per unit weight of adsorbent at equilibrium (mg/g), q_m is

amount of adsorbate adsorbed per unit weight of adsorbent required for monolayer adsorption (mg/g) and K_L is amount of adsorbate adsorbed at equilibrium (L/mg). The plot between C_e and C_e/q_e facilitates the calculation of Langmuir constants.

The Freundlich isotherm is an empirical relation between the solute concentrations on the adsorbent surface to the solute concentration in the contact liquid. It is obtained by considering heterogeneous surface with a non-uniform distribution of heat of adsorption. It assumes logarithmic decline in the heat of adsorption with increase in the extent of adsorption. It also indicates exponential variation in distribution sites with respect to adsorption energy. It does not show sufficient limit for monolayer filling. The adsorption isotherm derived by Freundlich equation is given by Freundlich[34]:

$$\ln q_e = \ln K_F + \frac{1}{n}\ln C_e \quad \text{... (4)}$$

where, K_F and n are the constants. K_F indicates the adsorption capacity (L/mg) and n indicates intensity of the adsorbent. These constants K_F (L/mg) and $1/n$ (dimensionless, heterogeneity factor) can be calculated by plotting the graph between $ln\ C_e$ and $ln\ q_e$.

Redlich-Peterson isotherm is a hybrid (fusion) between Langmuir and Freundlich systems. It included 3 unknown parameters: K_R, a_R and β into an empirical isotherm. Numerator is from Langmuir system and has advantage of reaching Henry region at boundless infinite dilutions. Denominator has fusion of Langmuir-Freundlich forms. This isotherm reaches Freundlich model at higher concentrations and is in accordance with the lower concentration limit of the Langmuir equation. The Redlich-Peterson isotherm equation is given by Redlich and Peterson[35]:

$$\ln\left(K_R\frac{C_e}{q_e}-1\right) = \ln a_R + \beta \ln C_e \quad \text{... (5)}$$

where, K_R (L/mg) and a_R (L/mg) are Redlich-Peterson isotherm constants and β is the exponent between 0 and 1.

Radke-Prausnitz isotherm considered the effects of improved fit of Langmuir isotherm modelling for adsorption isotherms. It has 3 adjustable parameters: K_{RP}, k_{RP} and P. At higher concentrations, this isotherm becomes Freundlich isotherm. Radke-Prausnitz isotherm equation is given by Radke and Prausnitz[36]:

$$q_e = \frac{K_{RP}k_{RP}C_e^P}{K_{RP}+k_{RP}C_e^{P-1}} \quad \text{... (6)}$$

where K_{RP} (L/g) is Radke-Prausnitz isotherm constant, k_{RP} ((mg/g)/(mg/L)$^{1/P}$) is a constant in Radke-Prausnitz isotherm and P is a dimensionless constant.

The equilibrium data obtained by the adsorption of CV and MB dyes on ACS have been used for the testing of applicability of various isotherm models. The various isotherm constants obtained from calculations using M.S Excel are given in Table 2.

Choosing best-fit isotherm based on error analysis

To optimize and augment the design of an adsorption process for the removal of adsorbate, it is substantial to craft most appropriate connection for the equilibrium curves[24,28]. Various isotherm models have been used to describe the equilibrium characteristics for adsorption of CV and MB dyes by ACS at different temperatures. The altered error functions of non-linear regression basin namely Hybrid Fractional Error Function (HYBRID), Marquardt's Percent Standard Deviation (MPSD) and The Average Relative Error (ARE) were employed to evaluate the isotherm constants, relate them with the less accurate linearized and non-linearized analysis values and to find out the best-fit isotherm model. The values of these error functions are provided in Table 2.

The **HYBRID** error function[37] developed by Porter in 1999 improves the fit of the ARE method at low concentrations. It includes the number of degrees of freedom of the system (i), the number of data points (n) and the number of parameters (p) of the isotherm equation. It is given by the following equation:

$$HYBRID = \frac{100}{N-p}\sum_{i=1}^{N}\left[\frac{\left(q_{e,\exp}-q_{e,calc}\right)}{q_{e,\exp}}\right]_i \quad \text{... (7)}$$

The MPSD error function[38] developed by Marquardt in 1963 has been used to test the adequacy and accuracy of the model fit with the experimental and theoretical data for lower concentrations. Conferring to the number of degrees of freedom of the system (i), it is comparable to some esteems of a modified geometric mean error distribution. A derivative of MPSD is given by the following equation:

$$MPSD = 100\sqrt{\frac{1}{N-p}\sum_{i=1}^{N}\left(\frac{\left(q_{e,\exp}-q_{e,calc}\right)}{q_{e,\exp}}\right)_i^2} \quad \text{... (8)}$$

ARE function[39] developed by Kapoor and Yang in 1999 indicates a tendency to under or overestimate

the experimental data. It considers different factors to describe the magnitude of relative error, and each of these factors is related to the standard measure of relative error, the coefficient of variation and its average. It tries to minimize the fractional error distribution across the complete concentration range. It is given by the following equation:

$$ARE = \frac{100}{N}\sum_{i=1}^{N}\left|\frac{\left(q_{e,\exp} - q_{e,calc}\right)}{q_{e,\exp}}\right|_i \quad \ldots (9)$$

where, q_e is the amount of adsorbate adsorbed per unit weight of adsorbent at equilibrium in mg/g, $q_{e,cal}$ is the calculated value of solid phase concentration of adsorbate at equilibrium in mg/g, $q_{e,exp}$ is the experimental value of solid phase concentration of adsorbate at equilibrium in mg/g. i is the number of degrees of freedom of the system, N is the number of data points and p is the number of parameters of the isotherm equation.

The values of the constants of all isotherm plots, the linear and nonlinear regression coefficient (R^2) are shown in Table 2. By comparing the results it is found that the Redlich-Peterson isotherm is best-fitted the isotherm data for CV and MB dyes adsorption on ACS at almost all temperatures. It may, however, be noted that the error analysis values and the non-linear correlation coefficients, R^2 are comparable for all other isotherms. Hence any one of the isotherms could be used for CV and MB dyes adsorption on ACS. Similarly, the error values of HYBRID, MPSD and ARE are lowest for the Redlich-Peterson isotherm. The plots for the Redlich-Peterson isotherm for CV and MB dyes adsorption on ACS fitting the experimental data at different temperatures are shown in Fig. 10(a and b) respectively.

Thermodynamic study

The increase in adsorption of CV and MB dyes with temperature indicates that adsorption processes of both dyes were endothermic. This can be explained thermodynamically by evaluating the parameters such as change in enthalpy (ΔH^0), change in entropy (ΔS^0) and change in Gibbs free energy (ΔG^0). According to chemist Jacobus Van't Hoff chemical thermodynamics for a given chemical reaction determine the internal heat energy, enthalpy, and entropy and free energy values of the system during chemical or physical transformation and inspect how they are dependent on to the reaction conditions[40]. Inspection of the thermal parameters that accompany chemical reactions and the thermal properties of the reactants like change in entropy (ΔS^0) and enthalpy (ΔH^0) could make it possible to lay forward a general measure about the spontaneity of the reaction and helps to obtain information about the equilibrium.

The Gibbs free energy change (ΔG^0) is related to the adsorption equilibrium constant by the standard Van't Hoff equation:

$$\Delta G^0 = -RT\ln K \quad \ldots (10)$$

According to thermochemistry, the Gibbs free energy change (ΔG^0) is also related to the change in entropy (ΔS^0) and heat of adsorption (ΔH^0) at fixed temperature. It is shown by the following equation:

$$\Delta G^0 = \Delta H^0 - T\Delta S^0 \quad \ldots (11)$$

Combining the above two equations, result in the following equation:

$$\ln K = \frac{-\Delta G^0}{RT} = \frac{\Delta S^0}{R} - \frac{\Delta H^0}{R}\frac{1}{T} \quad \ldots (12)$$

where, K indicates single point or distribution coefficient and is the ratio of q_e to C_e, ΔG^0 indicates the free energy change in kJ/mol, ΔH^0 indicates the change in enthalpy in kJ/mol, ΔS^0 indicates the change in entropy in kJ/mol K, T indicates the absolute temperature in K and R indicates the universal gas constant i.e. 8.314 J/mol.K. Thus thermodynamic parameter ΔH^0 can be determined by the slope of the linear Van't Hoff plot i.e. as ln$K$ versus ($1/T$), using equation:

$$\Delta H^0 = \left[R\frac{d\ln K}{d\left(1/T\right)}\right] \quad \ldots (13)$$

Fig. 12 shows that the Van't Hoff's plot of lnK as a function of $1/T$, gives a straight line with negative slope with the $R^2 = 0.755$ for CV and $R^2 = 0.830$ for MB from which the values of ΔH^0, ΔS^0, and ΔG^0 have been calculated. The values of ΔH^0, ΔS^0, and ΔG^0 at all temperatures is given in Table 3 for adsorption of CV and MB dyes onto ACS. ΔH^0 and ΔS^0values for adsorption of both CV and MB dyes were calculated from the slopes and intercepts, respectively (Fig. 12).

The results of thermodynamic parameters are given in Table 3. The positive values of ΔH^0 for CV (28.10 kJ/mol) and MB (33.52 kJ/mol) confirm the endothermic nature of the overall adsorption process[41]. The adsorption process in the solid-liquid

structure is a combination of two processes, firstly, desorption of the solvent i.e. water formerly adsorbed and secondly, adsorption of adsorbate species. The CV and MB ions have to transfer more than one water molecule for their adsorption and this result in the endothermicity of the adsorption process. The positive values of ΔS^0 (0.194 kJ/mol K for CV and 0.220 kJ/mol K for MB) show the affinity of adsorbent (ACS) and indicate that the two systems have an increased randomness at the solid-liquid interface with some structural changes in the adsorbate and adsorbent and an affinity of the ACS towards CV and MB. Also, positive ΔS^0 value corresponds to rise in the degree of freedom of the adsorbed species[42]. The values of Gibbs free energy changes (ΔG^0) for adsorption of both CV and MB were found to be negative. The negative ΔG^0 values prove that adsorption of both CV and MB dyes was spontaneous and decline in ΔG^0 values with increasing temperature reflects that the adsorption process is more applicable at higher temperatures.

Adsorption kinetics study

The kinetic adsorption considers the solute uptake rate of the adsorbent that in turn governs the equilibrium time of adsorption reaction. In the present work, adsorption kinetic study is carried out in batch (Fig. 13(a and b) and Fig. 14(a and b)) to investigate the controlling mechanism of adsorption process such as chemical reactions and mass transfer. The pseudo-first-order and pseudo second order kinetic equations are applied to model kinetics of CV and MB adsorption onto ACS. The samples containing CV-ACS and MB-ACS were taken in 250 mL stoppered glass conical flask. The samples were tested for a time period of 5 to 320 min at 303K for initial

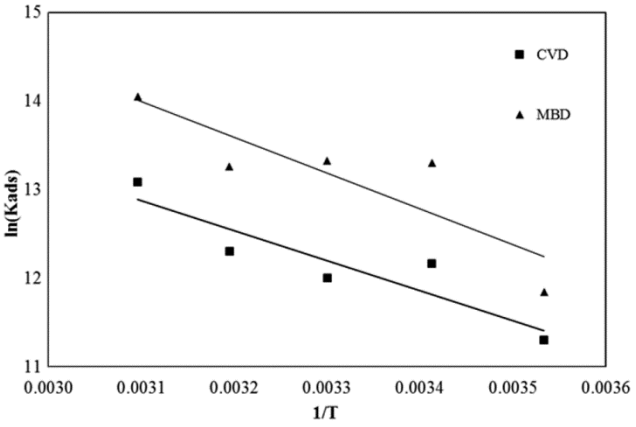

Fig. 12 — Van't Hoff's plot of ACS sorption distribution coefficient.

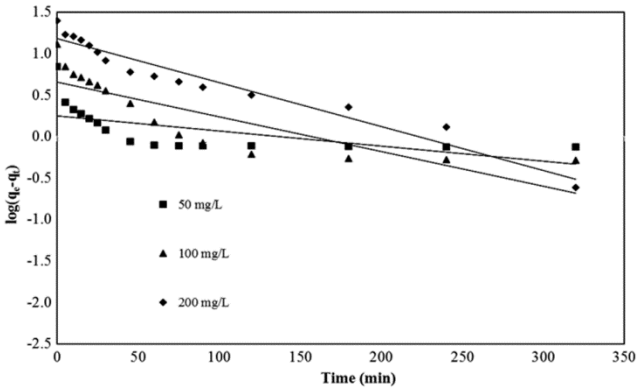

(a)

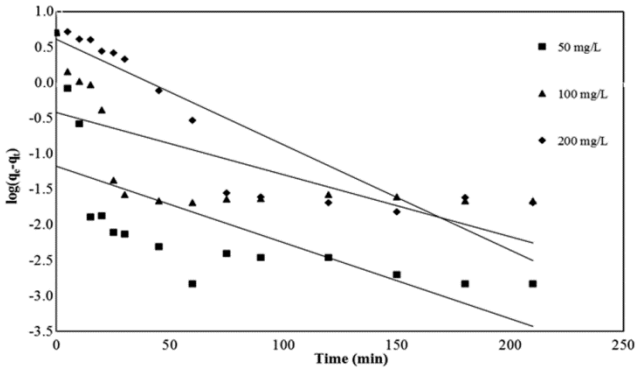

(b)

Fig. 13(a-b) — (a) Pseudo 1st order Equation Graph for Kinetic Study on CV-ACS (C_0 = 50, 100 and 200 mg/L, V = 50 mL, m = 8 g/L, pH_0 = 6.51, T = 303K and RPM = 150) and (b) Pseudo 1st order Equation Graph for Kinetic Study on MB-ACS (C_0 = 50, 100 and 200 mg/L, V = 50 mL, m = 10 g/L, pH_0 = 6.96, T = 303K and RPM = 150).

Table 3 — Thermodynamic parameters for adsorption of CV and MB dyes by ACS at various temperatures (t = 1 hour, C_0= 100-500 mg/L, m_{CV}= 8 g/L and m_{MB}= 10 g/L, RPM = 150).

Temperature (K)	K (L/g)		ΔG^0 kJ/mol		ΔH^0 kJ/mol		ΔS^0 kJ/mol	
	CV	MB	CV	MB	CV	MB	CV	MB
283	80.90	139.80	-26.84	-28.81	28.10	33.52	0.194	0.220
293	193.11	598.39	-28.78	-31.01				
303	163.41	612.93	-30.73	-33.22				
313	220.14	573.21	-32.67	-35.42				
323	484.08	1266.79	-34.61	-37.62				

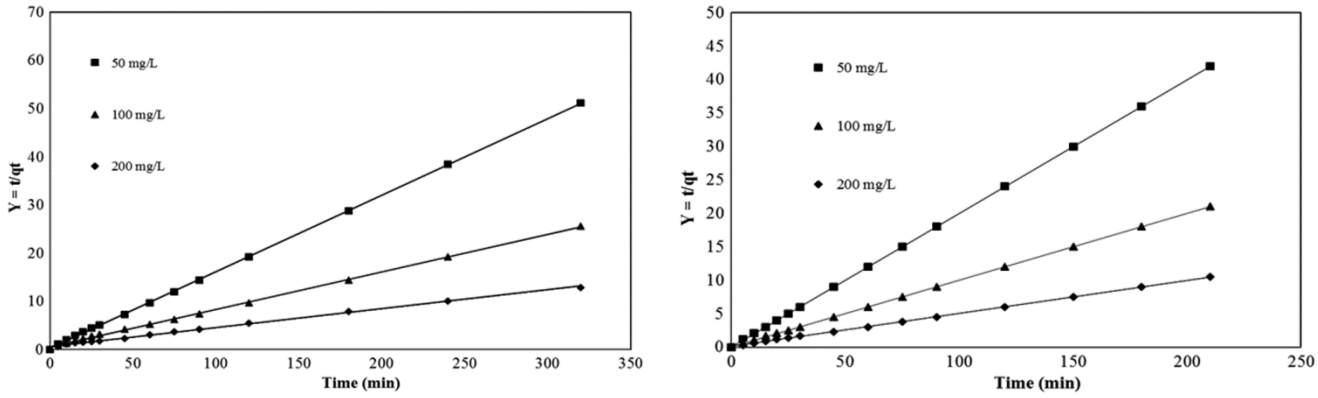

Fig. 14(a-b) — (a) Pseudo 2nd order Equation Graph for Kinetic Study on CV-ACS (C_0 = 50, 100 and 200 mg/L, V = 50 mL, m = 8 g/L, $p\mathrm{H}_0$ = 6.51, T = 303K and RPM = 150) and (b) Pseudo 2nd order Equation Graph for Kinetic Study on MB-ACS (C_0 = 50, 100 and 200 mg/L, V = 50 mL, m = 10 g/L, $p\mathrm{H}_0$ = 6.96, T = 303K and RPM = 150).

Table 4 — Kinetic parameters for removal of CV and MB dyes by ACS for pseudo first and pseudo second order kinetics:

pseudo first order kinetics:								
Concentration (mg/L)	$q_{e,exp}$ (mg/g)		$q_{e,cal}$ (mg/g)		k_f		R^2	
	CV	MB	CV	MB	CV	MB	CV	MB
50	6.212	4.999	1.761	0.066	0.004	0.025	0.381	0.452
100	11.504	9.990	4.567	0.382	0.010	0.020	0.711	0.424
200	19.686	19.704	15.118	4.101	0.012	0.034	0.942	0.787
pseudo second order kinetics:								
Concentration (mg/L)	$q_{e,exp}$ (mg/g)		$q_{e,cal}$ (mg/g)		k_s		R^2	
	CV	MB	CV	MB	CV	MB	CV	MB
50	6.212	4.999	6.301	5.008	0.079	0.849	0.999	1.000
100	11.504	9.990	12.853	10.030	1.759	0.179	0.999	1.000
200	19.686	19.704	25.445	20.284	0.002	0.020	0.996	0.999

dye concentrations of 50, 100 and 200 mg/L. The volume of sample taken was 50mL, optimum dosage (m_{CV} = 8 g/L and m_{MB} = 10 g/L,), $p\mathrm{H}_0$ ($p\mathrm{H}_{0CV}$ = 6.51 and $p\mathrm{H}_{0MB}$ = 6.96), and agitation speed (150 RPM) are kept constant for this study. The equation for the pseudo first order kinetic is given as[43]:

$$\log(q_e - q_t) = \log(q_e) - \frac{k_f}{2.303}t \quad \text{... (14)}$$

where, k_f is the forward rate constant for the pseudo first order kinetics equation; q_e is the amount of adsorbate adsorbed per unit adsorbent at equilibrium, q_t is amount of adsorbate adsorbed per unit adsorbent at time t and t is the time of testing. Straight line plots (Fig. 13 a and b) of log (q_e - q_t) verses time (t) of the pseudo first order reaction were used to determine the rate constant k_f and correlation coefficients R^2 for different CV and MB concentrations. The pseudo first order equation is fit for the initial time period of the adsorption process. Table 4 shows the constants that are calculated from the pseudo first order kinetic graph. The pseudo first order kinetic model shows low R^2 values for both CV and MB with poor fitting and notable variances between the experimental and theoretical uptakes.

The equation for the Second order kinetic equation is given as[43]:

$$\frac{t}{q_t} = \frac{1}{k_s q_e^2} + \frac{1}{q_e}t \quad \text{... (15)}$$

where k_s is the forward rate constant for the second order kinetics equation, q_e is the amount of adsorbate adsorbed per unit adsorbent at equilibrium q_t is amount of adsorbate adsorbed per unit adsorbent at time t and t is the time of testing.

The linearized plots (Fig. 14 a and b) t/qt versus time (t) of the pseudo second order reaction at different CV and MB concentrations by ACS were

used to determine the rate constant k_s and correlation coefficients R^2. Table 4 shows the constants that are calculated from the pseudo second order kinetic graph. The plot of *t/qt* versus *t* for pseudo second order model yields very good straight lines (correlation coefficient, $R^2 \geq 0.999$) as compared to the plot of pseudo first order. The R^2 values are approximately close to unity. It is also seen that as the initial dye concentration increases, the q_e values goes on increasing. The pseudo second-order model fits the experimental data quite well and the theoretical and experimental uptakes are in good concurrence. The pseudo second order equation is a fit for the total time period of the adsorption process. These facts suggest that the adsorption of CV and MB dyes by ACS follows the pseudo-second-order kinetic model, which relies on the assumption that chemical adsorption may be the rate limiting step[44]. In chemisorption, the dye ions stick to the adsorbent surface by forming a chemical (usually covalent) bond and tend to find sites that maximize their coordination number with the surface[45].

The data obtained for the adsorption of CV and MB dyes using ACS following the pseudo second order kinetic model indicates that the CV and MB adsorption process appears to be controlled by the chemisorption process. This chemical adsorption may be because of functional groups on the surface of ACS and hydrogen binding between the hydroxyl group of CV and MB, and this may be a rate limiting step[44].

Conclusion

The present study shows that ACS can be used as an effective low cost adsorbent for the removal of CV and MB dyes from waste water. The physico chemical properties of ACS viz., moisture content, ash content, volatile matter and fixed carbon content of ACS are 17.60, 9.60, 17.00 and 55.80% respectively. The surface area and pore volume of ACS is found to be 737.76 m^2/g and 0.2582 cc/g respectively. SEM analysis show large number of asymmetrical porous cavities and lingo cellulosic honey comb like structure and there is distortion of pores and filled voids, and scale like layered deposition on the surface of ACS loaded with CV and MB respectively making the surface smooth and even compared with virgin ACS. FTIR spectra of virgin ACS and ACS loaded with dyes indicates the presence of distinct functional groups like O-H, C-H, C-C, C-O etc. on the surface of ACS. The optimum adsorbent dosage are found to be 8 g/L and 10 g/L for CV and MB respectively. Optimum *p*H for the removal of CV and MB was found to be 6.51 and 6.96 respectively. The Effect of initial dye concentration for removal of ACS shows that, the % removal of CV and MB decreases with increase in CV and MB concentrations. However, the amount of dyes adsorbed per unit adsorbent is increased for CV and MB both. The increase in dye adsorbed per unit gram of adsorbent with increasing temperature shows endothermic nature of adsorption process. From isotherm analysis and by comparing the results of the error functions values, it is found that Redlich-Peterson equation is best-fitted the isotherm data for CV and MB adsorption on ACS at almost all temperatures. Thermodynamic parameters ΔG^0, $\Delta H^0$and ΔS^0 at 303 K by for CV-ACS are found to be -42.99, 9.779, 0.174 kJ/mol and for MB-ACS are found to be -48.27, 35.043, 0.266 kJ/mol respectively. The positive value of ΔH^0 confirms the endothermic nature of the overall-sorption process. The positive value of ΔS^0 suggests increased variance and randomness at the solid/solution interface with some structural changes in the adsorbate and adsorbent and an affinity of the ACS towards CV and MB. Also, positive ΔS^0 value corresponds to rise in the extent of freedom of the adsorbed species. ΔG^0 values are negative indicating that the sorption process led to a decrease in Gibbs free energy. Negative ΔG^0 indicates the feasibility and spontaneity of the adsorption process. The kinetic study indicates that the pseudo second order kinetic equation is applicable for the entire process. Hence ACS can be used as an effective adsorbent for the removal of harmful and toxic impurities like dyes from the municipal and industrial water and waste waters.

References

1 Banat I M, Nigam P, Singh D & Marchant R, *Biores Tech,* 58 (1996) 217.

2 Allen S J, Mckay G & Porter J F, *J Colloid Interf Sci,* 280 (2004) 322.

3 Bhatnagar, A & Jain A K, *J Colloid Interf Sci,* 281 (2005) 49.

4 Rathi A K A & Puranik, S A, *Indian J Chem Technol,* 10 (1999) 670.

5 Singh K, Lataye D H & Wasewar K L, *ASCE, J Hazard Toxic Radioact Waste,* 20 (2016) 1.

6 Ingole R S & Lataye D H, *ASCE, J Hazard Toxic Radioact Waste,* 19 (2015) 1.

7 Dhorabe P T, Lataye D H & Ingole R S, *Water Sci Tech,* 73 (2016) 955.

8 Malwade K, Lataye D, Mhaisalkar V, Kurwadkar S & Ramirez D, *Int J Environ Sci Technol,* 13 (2016) 2107.

9 Velmurugan P, Kumar R V & Dhinakaran G, *Int J Environ Sci,* 1 (2011) 1492.

10 Singh K, Lataye D H & Wasewar K L, *J. Fluorine Chem.,* 194 (2017) 23.

11 Tay T, Erdem M, Ceylan B & Karago'z S, *Bioresources,* 7 (2012) 3175.

12 Dhorabe P T, Lataye D H & Ingole R S, *ASCE, J Hazard Toxic Radioact Waste,* 04016015 - 1 (2016) 1.

13 Theivarasu C, Mylsamy S & Sivakumar N, *Univers J Envi Res and Tech,* 1 (2011) 70.

14 Ingole R S, Lataye D H & Dhorabe P T, *KSCE, J Civ Eng,* 21 (2016) 100.

15 Crystal violet, *Wikipedia, the free encyclopedia,* (https://en.wikipedia.org/wiki/Crystal), 2016.

16 Reinhardt C & Travis A S, *Kluwer Acad. Dordrecht Netherland,* 1 (2000) 208.

17 Gessner T & Mayer U, *Triarylmethane and Diarylmethane Dyes,* Vol 1 - 6th Edition (Ullmann's Encyclopedia of Industrial Chemistry, Weinheim: Wiley-VCH), 2002.

18 Ahmad R, *J Hazard Mater,* 171 (2009) 767.

19 Methylene blue, *Wikipedia, the free encyclopedia,* (https://en.wikipedia.org/wiki/Methylene_blue), 2016.

20 Boeningo M, *U.S Gov. Printing Off. DNHS (NIOSH) Washington DC pub.,* 1 (1994) 80.

21 Qada E N, Allen S J & Walker G M, *Chem Eng J,* 135 (2008) 174.

22 BIS, *Indian Standard methods of test for soil: Part 4 - Grain size analysis,* Part 4 IS2720- 2nd Edition (Bureau of Indian Standards, New Delhi, India), 1985.

23 BIS, *Indian standard methods of test for coal and coke: Part I - Proximate analysis,* Part I IS1350- 4th Edition (Bureau of Indian Standards, New Delhi, India), 1984.

24 Lataye D H, Mishra I M, & Mall I D, *Chem Eng J,* 138 (2008a) 35.

25 Mirhabibi A, Esfidari M & Babazadeh R, *J Coat Technol Res,* 73 (2007) 347.

26 Lataye D H, Mishra I M & Mall I D, *Ind Eng Chem Res,* 45 (2006) 3934.

27 Uddin Md, Tamez Md, Islam A, Mahmud S & Rukanuzzaman Md, *J Hazard Mater,* 164 (2009) 53.

28 Lataye D H, Mishra I M & Mall I D, *J Hazard Mater,* 154 (2008b) 858.

29 Arami M, Yousefi N, Limaee M & Niyaz Md, *Chem Eng J,* 139 (2008) 2.

30 Srivastava V C, *Chem Eng J,* 132 (2007) 267.

31 Srivastava V C, Swamy, M M, Mall, I D, Prasad, B & Mishra, I. M.. *Colloids Surf A Physicochem Eng Asp.,* 272 (2006) 89.

32 Bhattacharyya K G & Sharma A, *J Environ Manage,* 71 (2004) 217.

33 Langmuir I, *J Am Chem Soc,* 40 (1918) 1361.

34 Freundlich H M F, *J Phy Chem,* 57 (1906) 385.

35 Redlich O & Peterson D L, *J Phys Chem,* 63 (1959) 1024.

36 Radke C J & Prausnitz J M, AIChE, 18 (1972) 761.

37 Porter J F, McKay G & Choy K H, *Chem Eng Sci,* 54 (1999) 5863.

38 Marquardt D W, J Soc *Ind Appl Math,* 11 (1963) 431.

39 Kapoor A & Yang R T, *Gas Sep Purif,* 3 (1989) 187.

40 Van't Hoff J H, *Biography on Nobel prize,* (website, nobelprize.org. (1911-03-01)), 1911.

41 Gerc O, Gerc H F, Koparal, A S & Ogutveren U B, *J Hazard Mater,* 160 (2008) 668.

42 Raymon C, *Chemistry: Thermodynamic*, (McGraw-Hill, Boston), 1998.

43 Ho Y S & McKay G, *Process Biochem.,* 34 (1999) 451.

44 Xiaoli C & Youcai Z, *J Hazard Mater,* 137 (2006) 410.

45 Atkins P W, *Physical Chemistry,* Vol 1 - 5th Edition (Oxford University Press, Oxford), 1995.